AIRS Observed Stratospheric Cooling Rates Compared to Climate Models

2007 AIRS Science Team Meeting
March 27, 2007

Dan Feldman [1], Frank Li [2], Duane Waliser [2], Yuk Yung [3], Hartmut Aumann [2]

[1] Department of Environmental Science and Engineering, Caltech
[2] Jet Propulsion Laboratory
[3] Division of Geological and Planetary Sciences, Caltech

Introduction

- Stratosphere cooling is more rapid than the tropospheric warming due largely to increases of CO_2
- Brewer-Dobson circulation largely determines the O_3 spatial distribution.
  - Result of planetary wave activity
  - Affected by radiative processes including solar heating and infrared cooling
  - Circulation is strengthening with increased CO_2
- Understanding radiative heating/cooling rates is necessary for understanding the radiative control of circulation in the stratosphere.

Holton et al., 1995

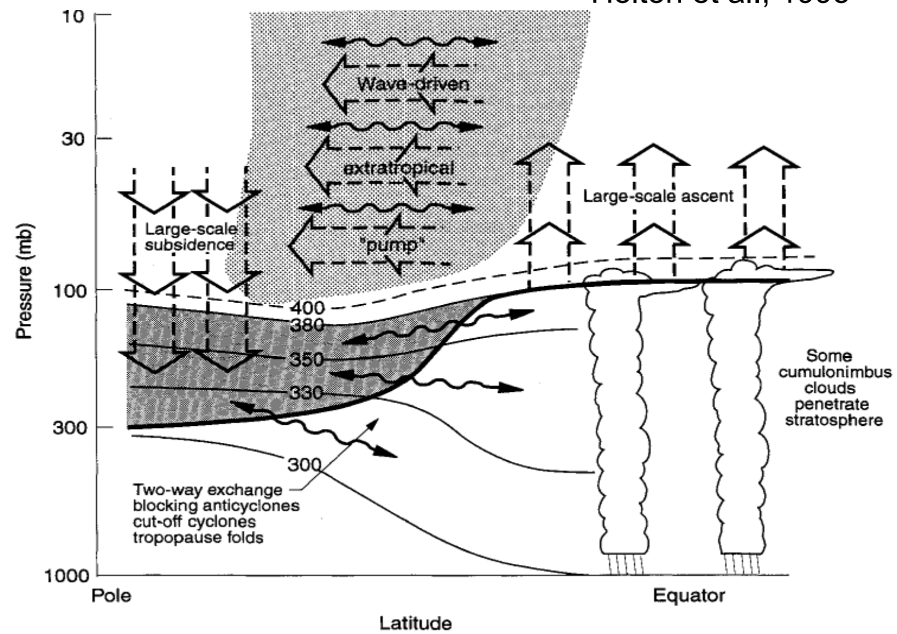

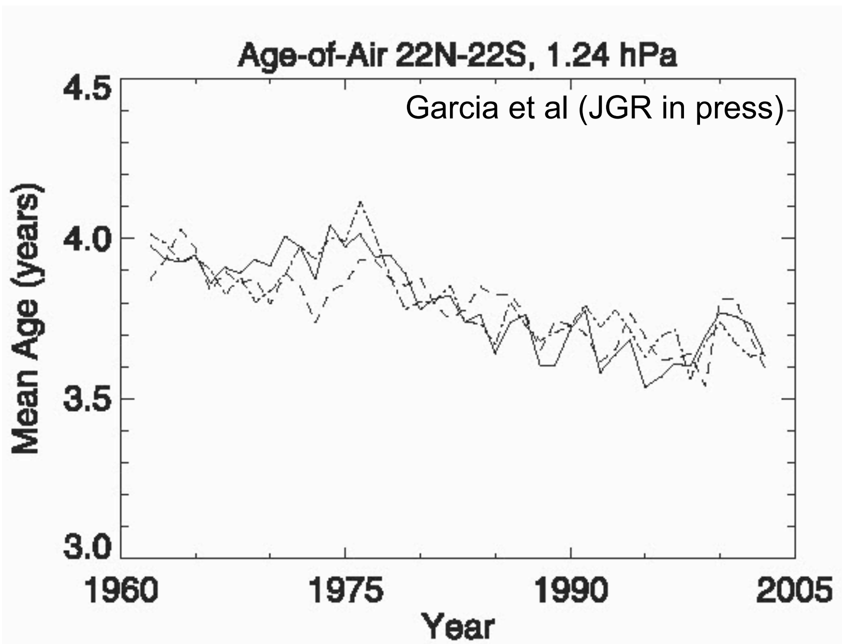

Cooling Rate Calculations

- Radiative heating/cooling rates directly proportional to net flux divergence in a layer
  - Upwelling surface flux
  - Flux from layers below
  - Flux from layers above
  - Layer emission, transmission
- Knowledge of T, H_2O, O_3 profiles required
- RRTM (Mlawer et al., 1997) utilized for fast RT calculations
  - ±0.1 K/day in trop. relative to line-by-line
  - ±0.3 K/day in strat. Relative to line-by-line

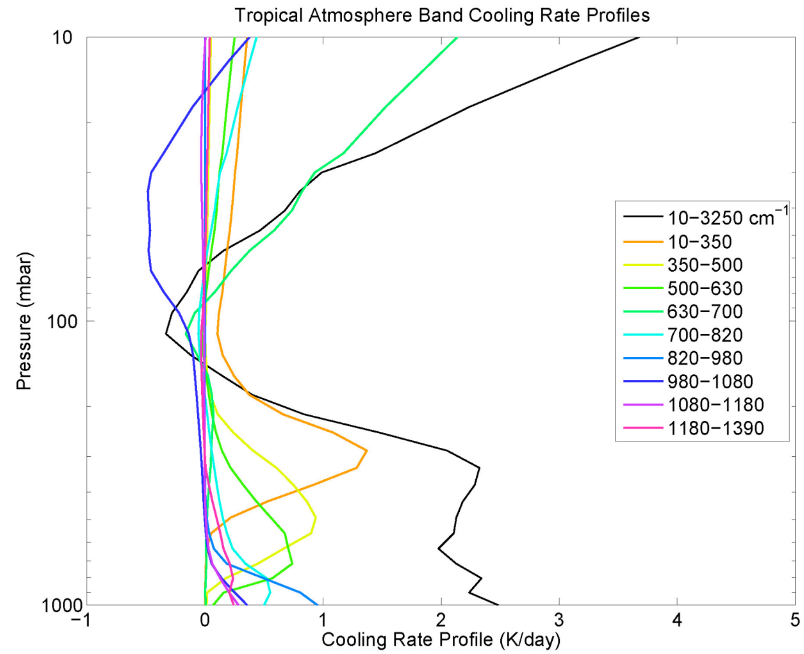

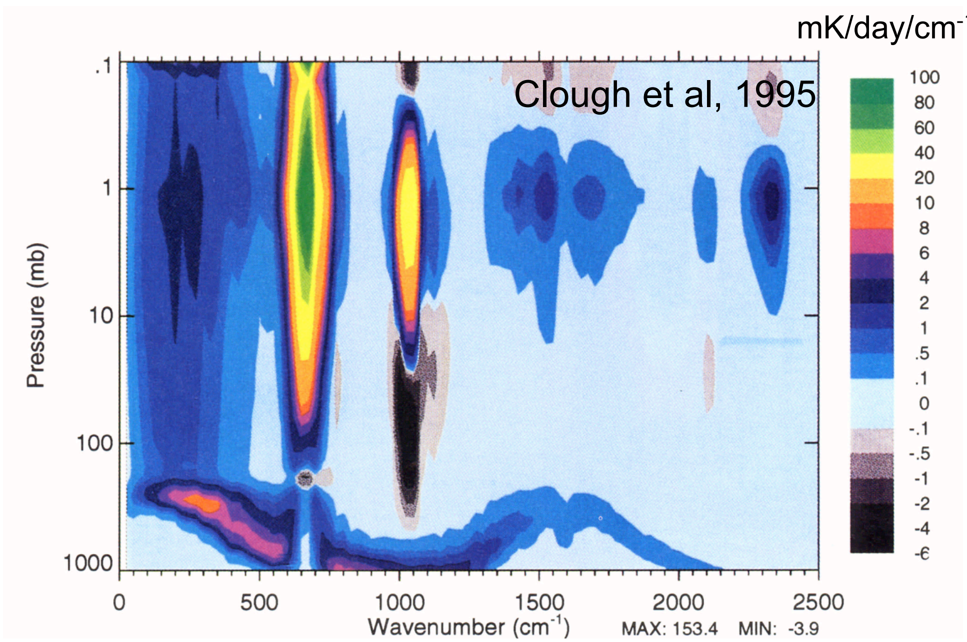

Cooling Rate Error Budget

- Perturbations in T, H_2O, O_3 in the layer of interest affect that layer's cooling rate but also affect cooling in adjacent layers
  - i.e. $\Delta T(z_L) > 0 \rightarrow \Delta\theta'(z_L) > 0$
    $\rightarrow \Delta\theta'(z_{L+1}) < 0$
    $\rightarrow \Delta\theta'(z_{L-1}) < 0$
- Formal error propagation analysis
  - Uncertainties in T(z), H_2O(z), and O_3(z) propagate into cooling rate profile uncertainty
  - Non-zero covariance in T(z), H_2O(z) and O_3(z) errors must be recognized
- CO_2, O_3 bands contribute substantially to *a priori* uncertainty

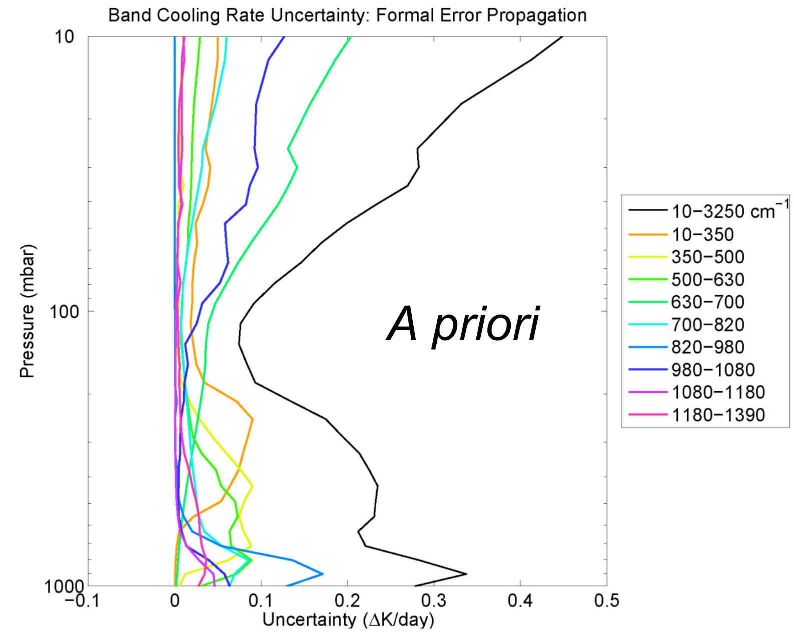

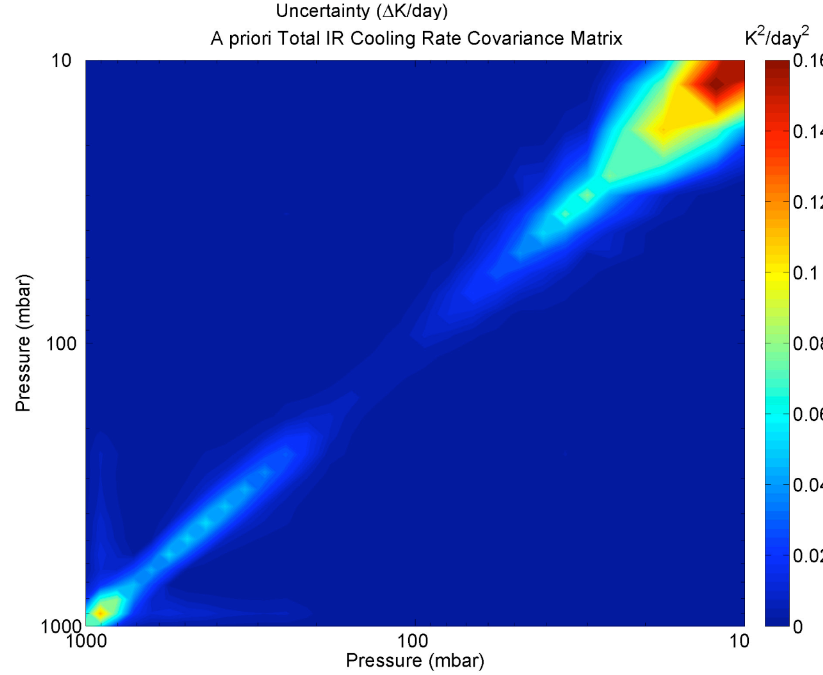

Why 50 mbar

- Small T trend allows for measurement/model inter-comparison
- T, O_3 averaging kernels for linear Bayesian retrieval are narrow
  - H_2O ambiguity in AIRS signal at 50-mbar

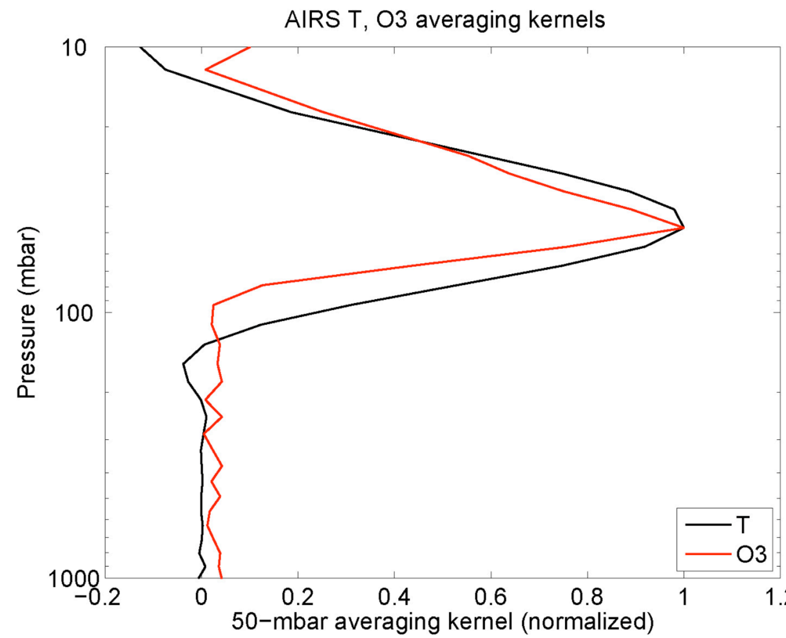

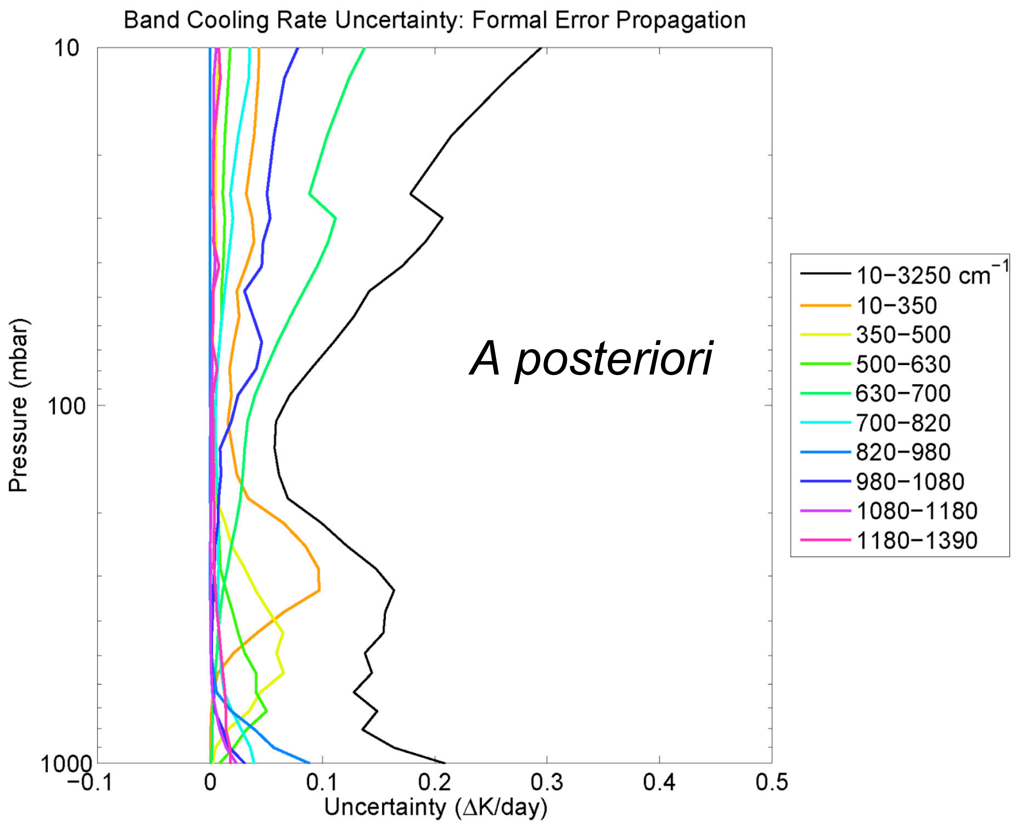

- Cooling rate error at 50 mbar after AIRS measurement ~0.15 K/day, mostly from CO_2, O_3 bands

AIRS: a Tool for Cooling Rate Profile Analysis

- AIRS measurements contain information regarding radiative cooling rates up to 10 mbar
  - Explicit through measurement of several bands:
    - CO_2 v_2
    - Window
    - O_3 v_3
    - H_2O v_3
  - Implicit (far-infrared H_2O rotational band)
  - Cooling from stratospheric H_2O not constrained by AIRS measurements
  - See Feldman et al. (2006) for intercomparison of cooling rates derived various measurements.
- Cloud top pressure and temperature and cloud fraction are sufficient to constrain stratospheric cooling rates
- For troposphere and tropopause layer, synergy with other instruments may allow for analysis of cooling rates and comparison with models.

AIRS L3 products at 50-mbar

- AIRS L3 T, H_2O, O_3, CTP, CTT, CLW products utilized (Olsen et al)
  - Several L3 months missing
- Expected features of 50-mbar temperatures and cooling rates derived from AIRS data
  - Cooling rate at 50-mbar follows but is not synced with temp. at 50 mbar

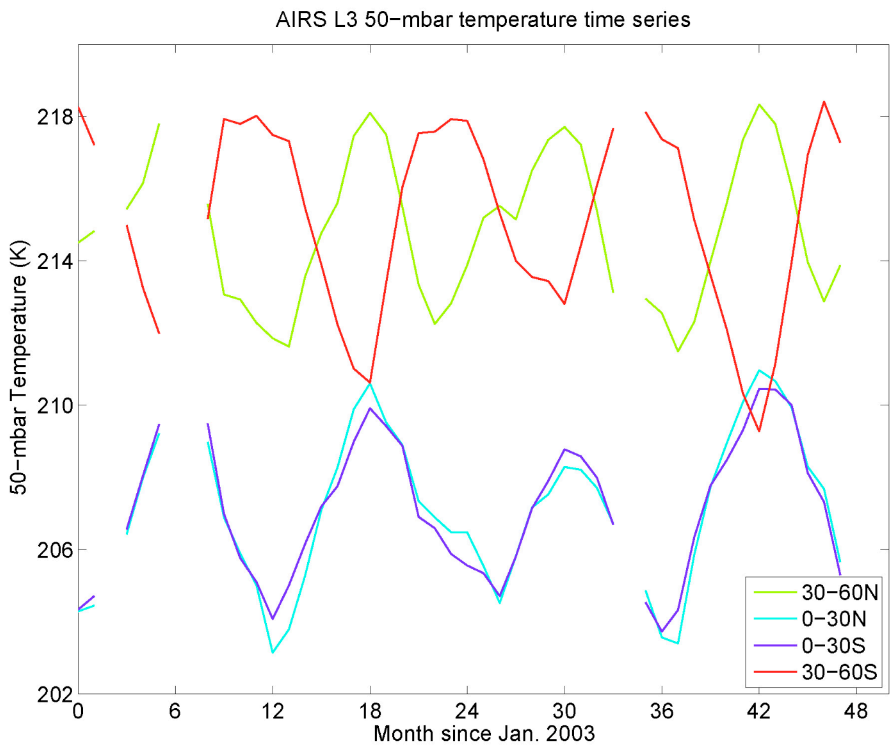

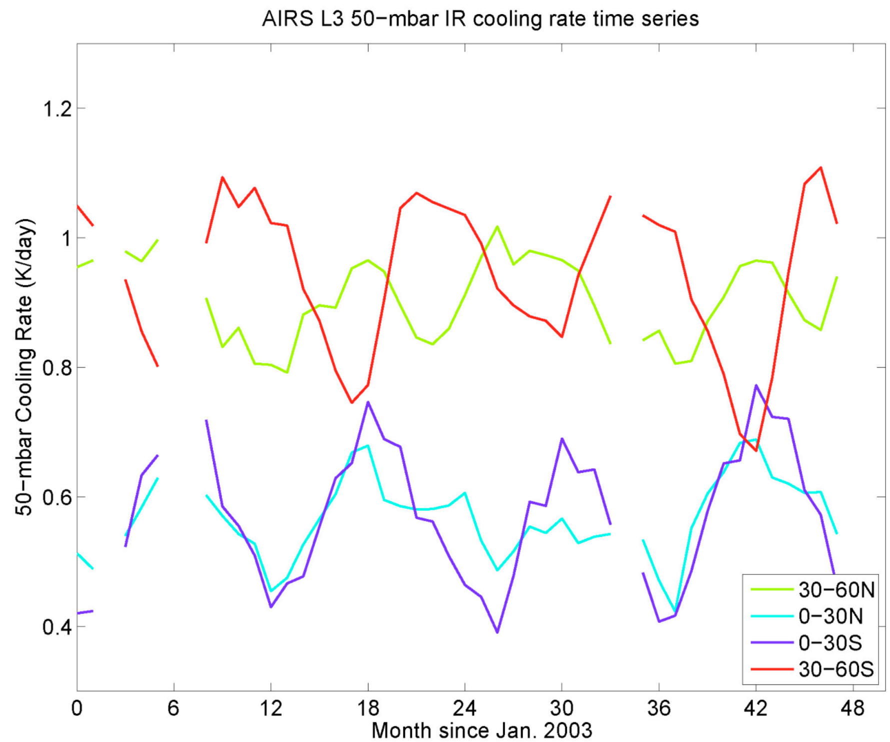

AIRS L3 50-mbar T and θ’ Selected Maps

- At 50-mbar cooling-to-space term dominates
- O_3 offsets CO_2 (and H_2O) cooling
  - O_3 profile knowledge necessary for accurate cooling rate determination

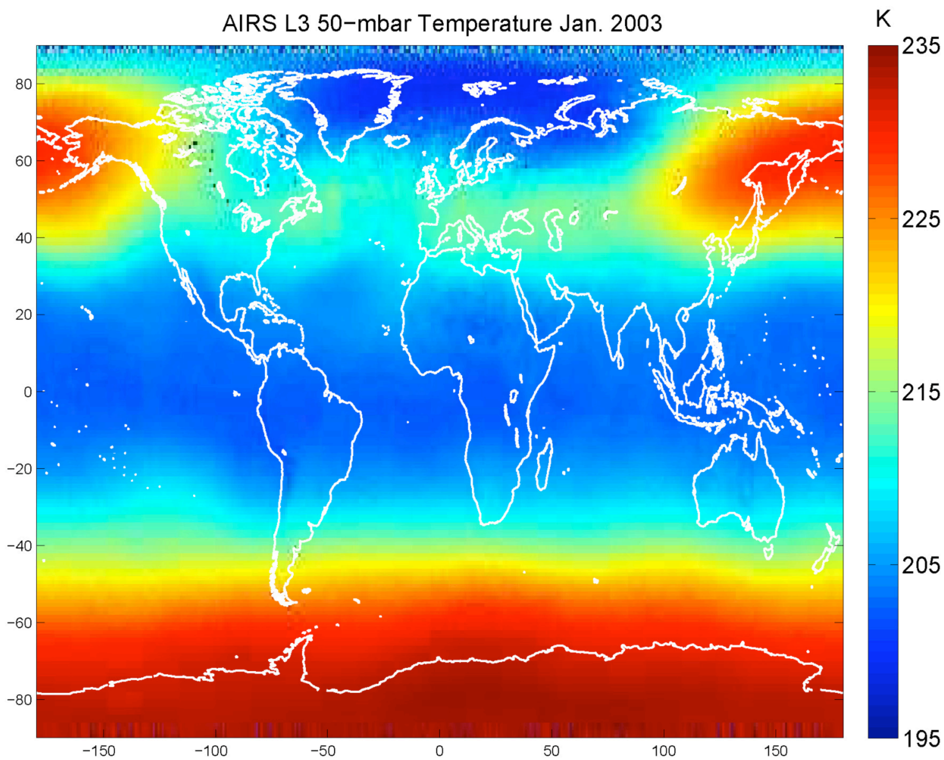

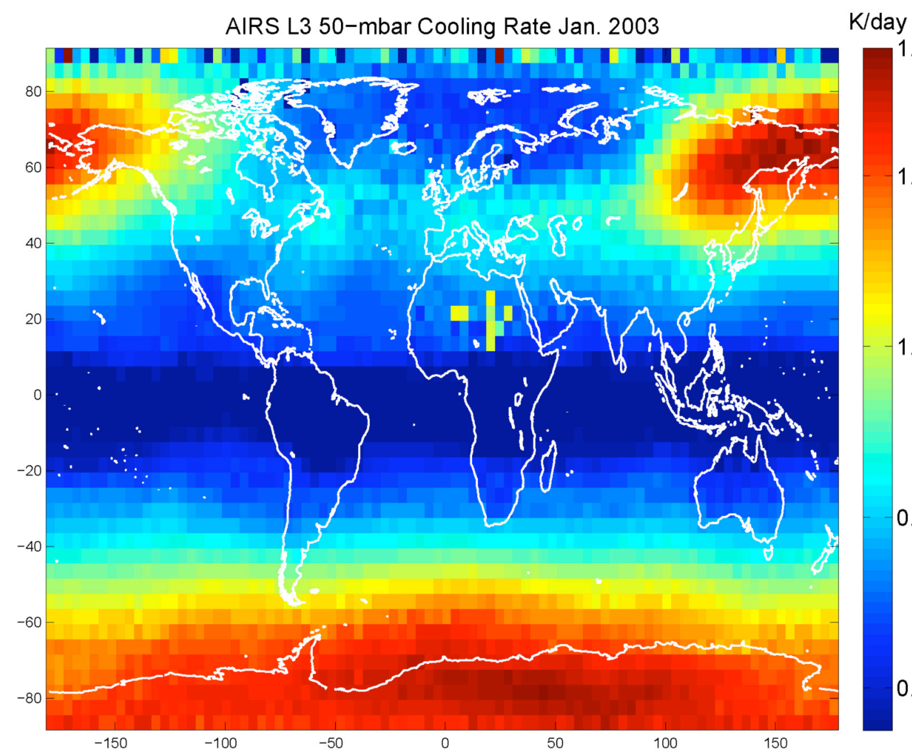

50-mbar T and θ’ differences

- AIRS and ERA-40 (Uppala et al) 50-mbar T and θ’ agree with some discrepancies in high-latitude winter hemisphere
- AIRS and GISS (Schmidt et al) have substantially more disagreement in T and θ’

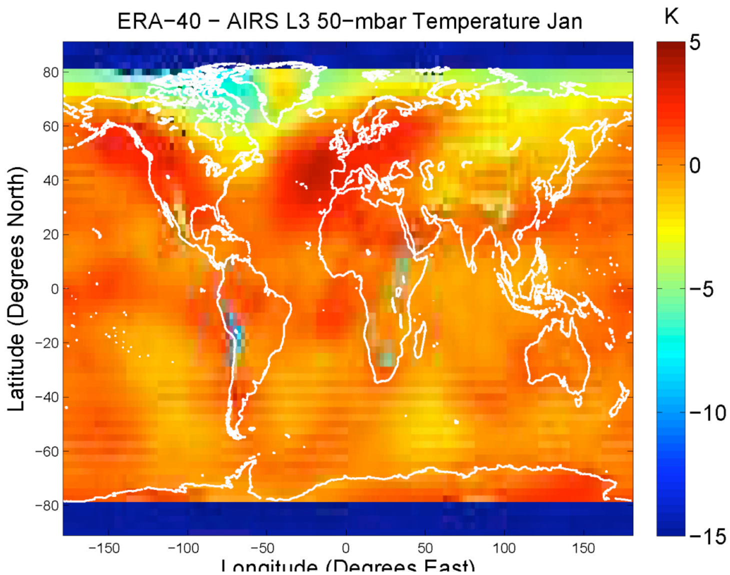

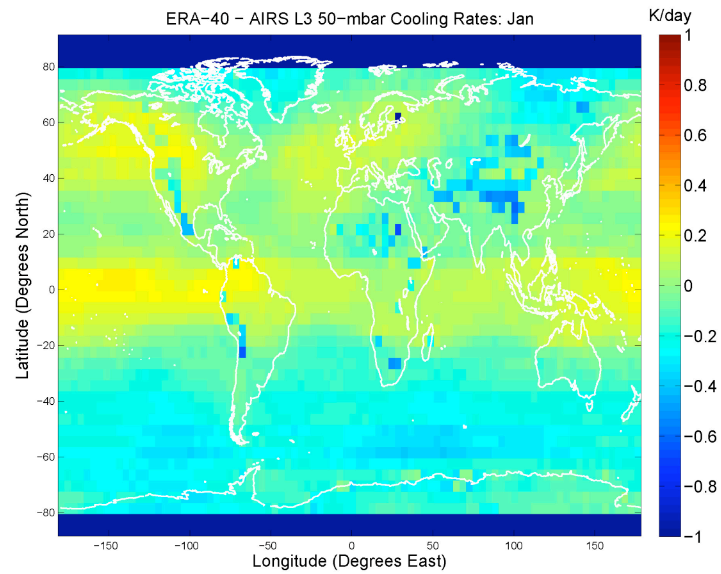

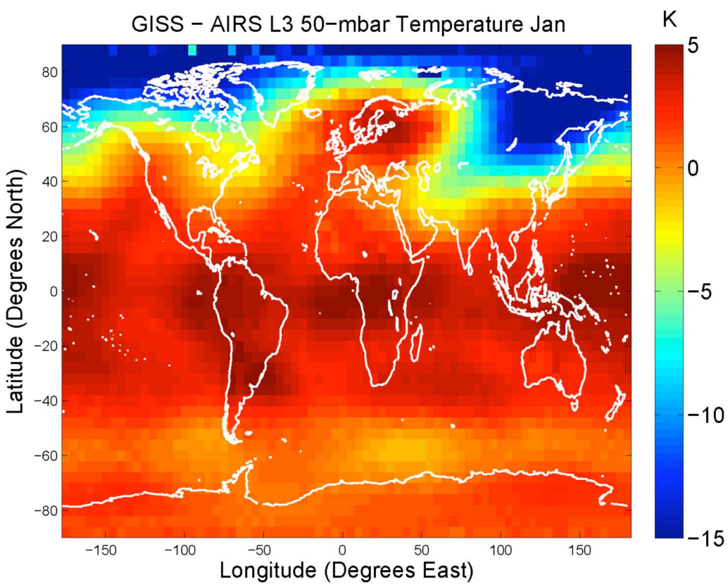

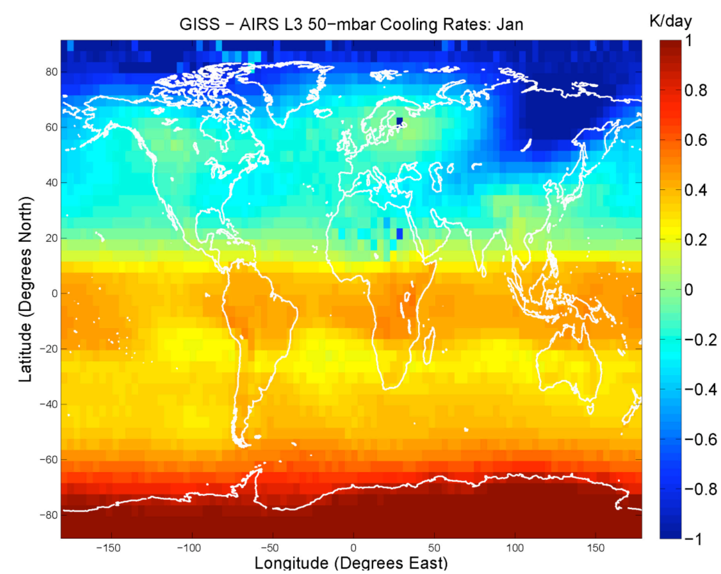

Phase (and amplitude) comparison of AIRS L3 with models and reanalysis

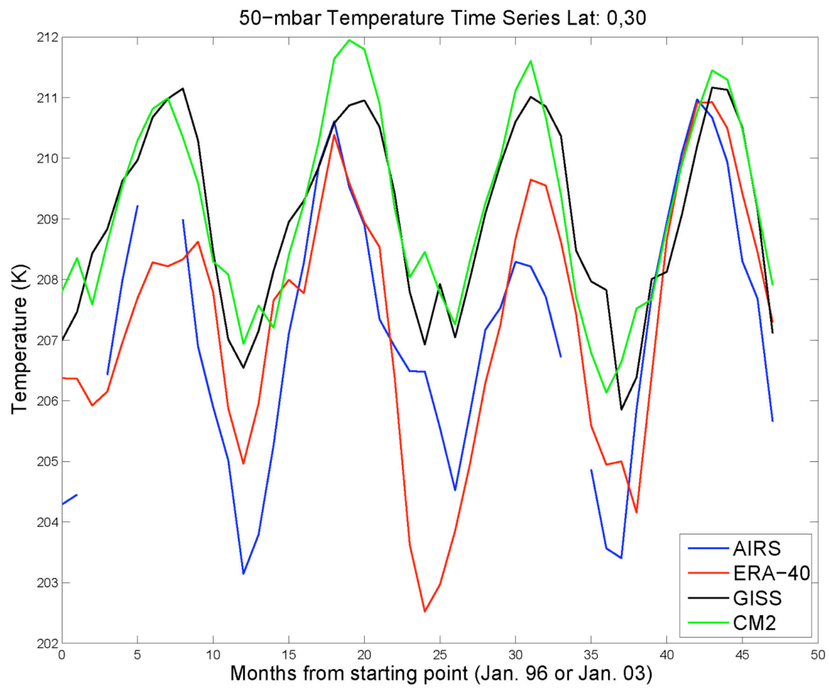

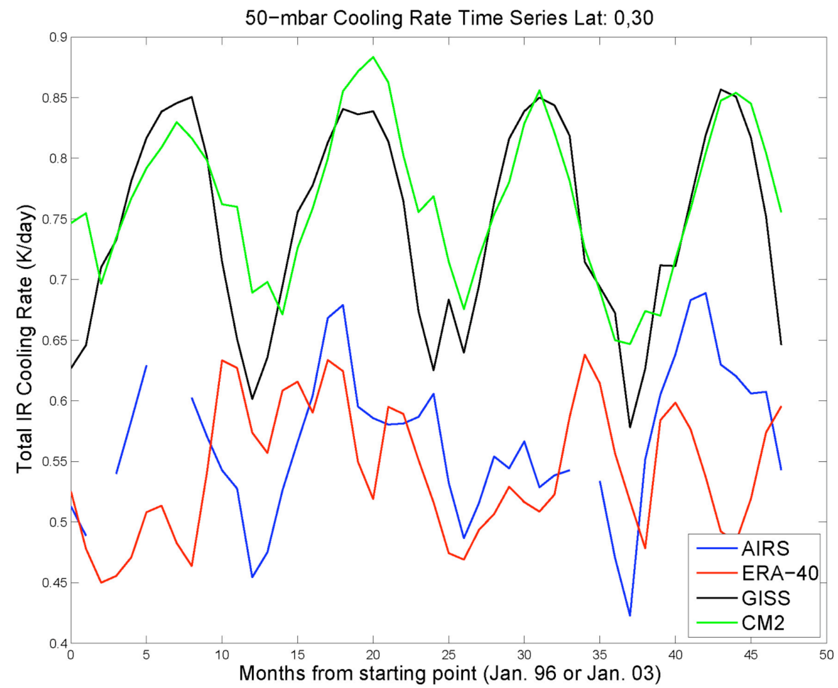

<u>Lags</u>	
ERA-40:	0.3 months
GISS:	1.3
CM2:	0.5

- Phase of 50-mbar signal:
  - the mean time each year when the signal crosses the mid-point between the maximum and the minimum on up-swing.

Conclusions

- Stratospheric T and θ' are necessary for determining stratospheric circulation
- AIRS measurements capture stratospheric cooling rates to within 0.15 K/day (within stated computational accuracy of band-model).
- Comparison between 50-mbar temperature and cooling rates from AIRS and models
  - AIRS data suggest phase of 50-mbar temperature in models lagging
  - Models predict warmer low-latitude, colder high-latitude mid-stratosphere than AIRS L3
  - Model cooling rates follow 50-mbar temperature deviation but hemispheric biases present.
- For a longer discussion of using thermal IR sounders for cooling rate analysis, look for Feldman et al (JGR in prep)

Acknowledgements

- NASA Earth Systems' Science Fellowship
  - Grant #: NNG05GP90H
- Yuk Yung's IR radiation group
- Kuo-Nan Liou (UCLA)
- Kuai Le (Caltech)

References

- Anderson, J.L. et al. (2004) The New GFDL Global Atmosphere and Land Model AM2-LM2: Evaluation with Prescribed SST Simulations, *Journal of Climate*, 17: 4641-4673.
- Clough, S.A., and M.J. Iacono (1995). Line-by-line calculation of atmospheric fluxes and cooling rates 2. Application to carbon dioxide, ozone, methane, nitrous oxide and the halocarbons. *Journal of Geophysical Research*, 100(D8): 16519-16535.
- Feldman, D.R., K.N. Liou et al. (2006). Direct retrieval of stratospheric CO_2 infrared cooling rate profiles from AIRS data, *Geophysical Research Letters*, 33: 2005GL024680.
- Garcia, R. R., D. R. Marsh, D. E. Kinnison, B. A. Boville, and F. Sassi (2007), Simulation of secular trends in the middle atmosphere, 1950–2003, *Journal of Geophysical Research*, 112, XXXXXX, doi:10.1029/2006JD007485.
- Holton, J.R., P.H. Haynes, et al. (1995), Stratosphere-Troposphere Exchange, *Review of Geophysics*, 33(4): 403-439.
- McClatchey, R.A., Fenn, R.W., Selby, J.E.A., Volz, F.E., Garing, J.S. (1971). "Optical properties of the atmosphere." ARCRL-71-0279, Air Force Geophysics Lab, Bedford, MA.
- Mlawer, E.J., Taubman, S.J., Brown, P.D., Iacono, M.J., Clough, S.A. (1997). "RRTM, a validated correlated-k model for the longwave." *Journal of Geophysical Research*. 102: 16,663-16,682.
- Olsen, E.T. et al. (2005). AIRS/AMSU/HSB Version 4.0 Data Release User Guide. http://daac.gsfc.nasa.gov/AIRS/documentation/v4_docs/V4_Data_Release_UG.pdf
- Rodgers, C. D. (2000). Inverse Methods for Atmospheric Sounding: Theory and Practice. London, World Scientific.
- Schmidt, G.A. et al. (2006). Present-Day Atmospheric Simulations Using GISS ModelE: Comparison to In Situ, Satellite, and Reanalysis Data. *Journal of Climate,* 19(2): 153-192.
- Uppala, S.M., Kållberg, P.W., Simmons, A.J., et al. (2005): The ERA-40 re-analysis. *Quarterly Journal of the Royal Meteorological Society*, 131, 2961-3012.

Cooling Rate Calculations

- Radiative heating/cooling rates directly proportional to net flux divergence in layer

Surface

Layers below

$$\dot{\theta}_{\bar{\nu}}(z) = \frac{2\pi}{\rho(z) C_p}\left[\varepsilon_{\bar{\nu}} B_{\bar{\nu}}\left(\theta\left(z_{surf}\right)\right) \frac{\partial T^f_{\bar{\nu}}(z_{surf}, z)}{\partial z} + \int_{z_{surf}}^{z} B_{\bar{\nu}}(z') \frac{\partial^2 T^f_{\bar{\nu}}(z', z)\, dz'}{\partial z' \partial z} - \int_{z}^{\infty} B_{\bar{\nu}}(z') \frac{\partial^2 T^f_{\bar{\nu}}(z', z)}{\partial z' \partial z} dz' \right]$$

Layers above

- Knowledge of T, H_2O, O_3 profile required
- RRTM utilized for fast RT calculations
  - ±0.1 K/day in trop. relative to LBLRTM
  - ±0.3 K/day in strat. Relative to LBLRTM

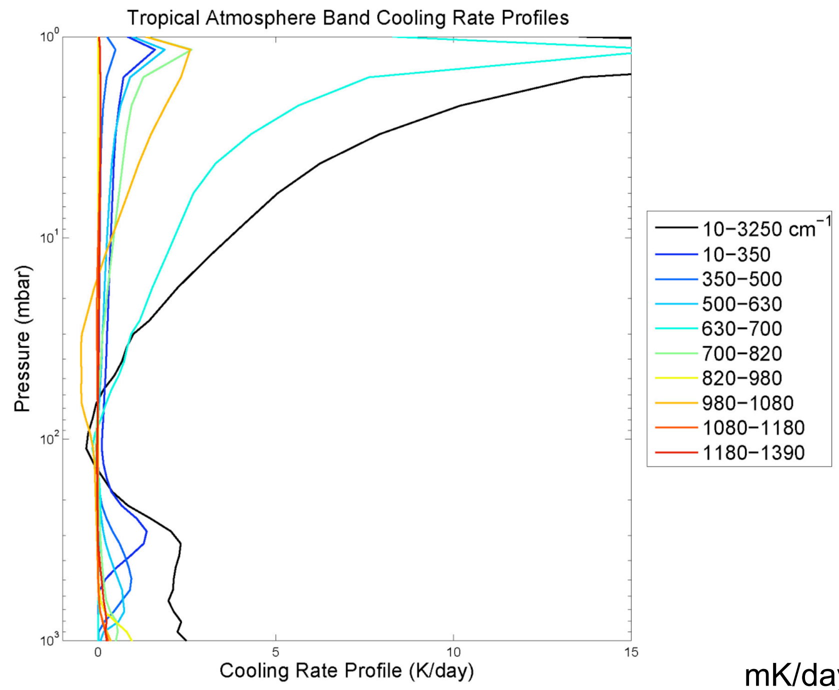

mK/day/cm^{-1}

Cooling Rate Error Budget

- Perturbations in T, H_2O, O_3 in the layer of interest affect that layer's cooling rate but also affect cooling in adjacent layers
  - i.e. $\Delta T(z_L) > 0 \;\rightarrow \Delta\theta(z_L) > 0$
    $\rightarrow \Delta\theta(z_{L+1}) < 0$
    $\rightarrow \Delta\theta(z_{L-1}) < 0$
- Formal error propagation analysis

$$\mathrm{var}\left[\Delta\dot{\theta}(z)\right] = \left\{ \begin{array}{l} \displaystyle\sum_{i=1}^{n}\left[\frac{\partial\dot{\theta}(z)}{\partial x_i}\right]^2 \mathrm{var}(x_i) + \\ \displaystyle\sum_{i=1}^{n-1}\sum_{j=i+1}^{n}\frac{\partial\dot{\theta}(z)}{\partial x_i}\frac{\partial\dot{\theta}(z)}{\partial x_j}\mathrm{cov}(x_i, x_j) \end{array} \right.$$

$$2\,\mathrm{cov}\left[\dot{\theta}(z_i), \dot{\theta}(z_j)\right] = \left\{ \begin{array}{l} \mathrm{var}\left[\dot{\theta}(z_i) + \dot{\theta}(z_j)\right] - \\ \mathrm{var}\left[\dot{\theta}(z_i)\right] - \mathrm{var}\left[\dot{\theta}(z_j)\right] \end{array} \right.$$

- CO_2, O_3 bands contribute substantially to *a priori* uncertainty

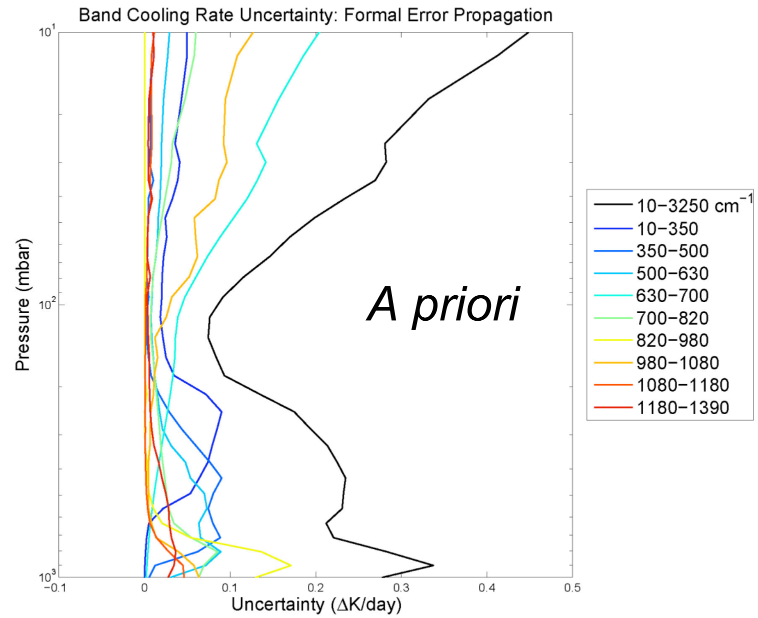

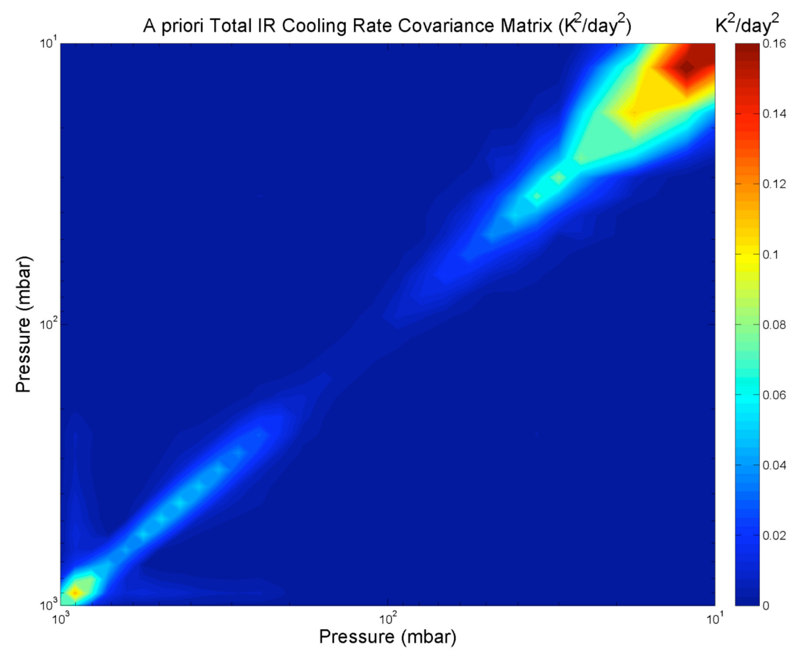

Phase comparisons for other latitude bands

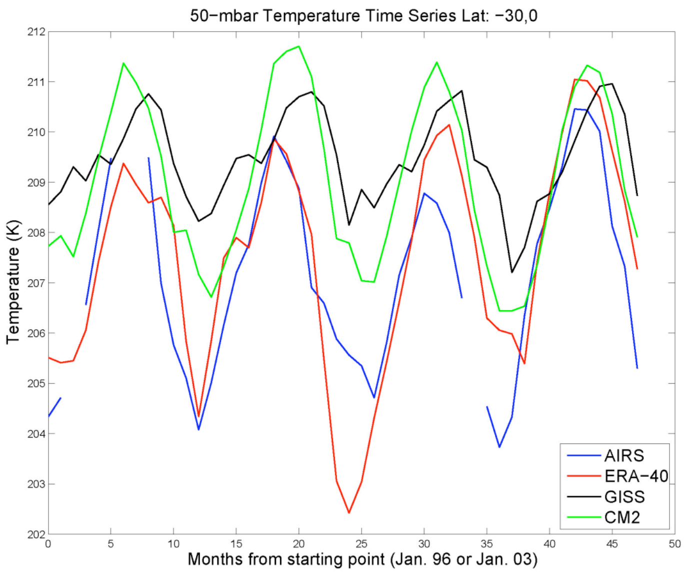

Lags:
ERA-40:
GISS:
CM2:

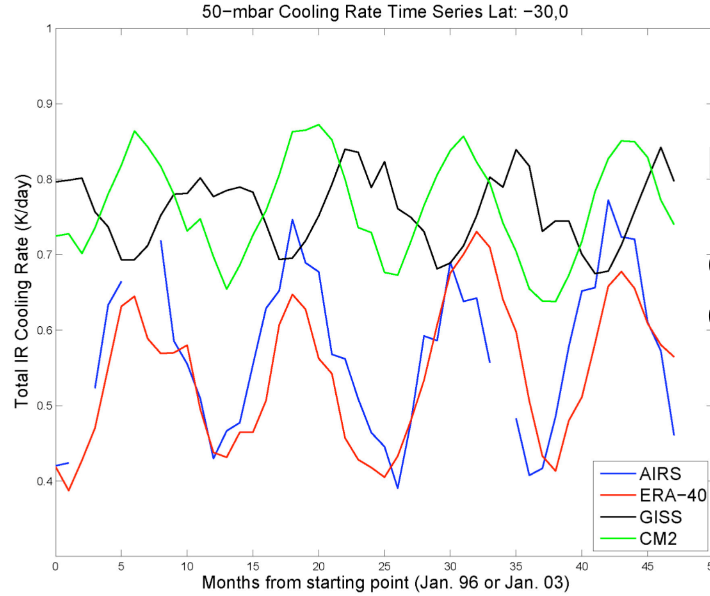

Lags:
ERA-40:
GISS:
CM2:

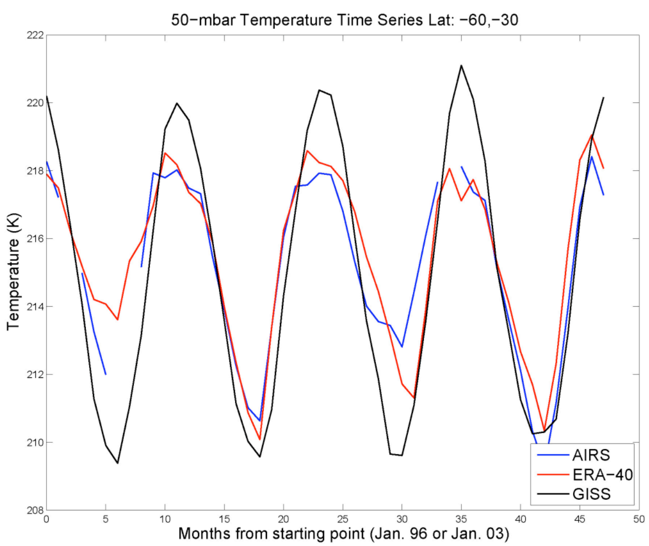

Lags:
ERA-40:
GISS:

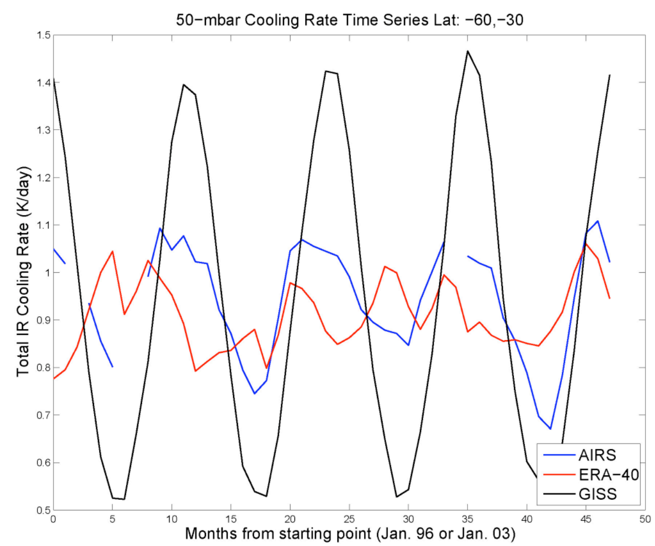

Lags:
ERA-40:
GISS: